Experimental Dendroclimatic Reconstruction of the Southern Oscillation

D. W. Stahle,* R. D. D'Arrigo,+ P. J. Krusic,+ M. K. Cleaveland,* E. R. Cook,+ R. J. Allan,# J. E. Cole,@ R. B. Dunbar,& M. D. Therrell,* D. A. Gay,* M. D. Moore,** M. A. Stokes,++ B. T. Burns,## J. Villanueva-Diaz,@@ and L. G. Thompson&&

ABSTRACT

Exactly dated tree-ring chronologies from ENSO-sensitive regions in subtropical North America and Indonesia together register the strongest ENSO signal yet detected in tree-ring data worldwide and have been used to reconstruct the winter Southern Oscillation index (SOI) from 1706 to 1977. This reconstruction explains 53% of the variance in the instrumental winter SOI during the boreal cool season (December–February) and was verified in the time, space, and frequency domains by comparisons with independent instrumental SOI and sea surface temperature (SST) data. The large-scale SST anomaly patterns associated with ENSO in the equatorial and North Pacific during the 1879–1977 calibration period are reproduced in detail by this reconstruction. Cross-spectral analyses indicate that the reconstruction reproduces over 70% of the instrumental winter SOI variance at periods between 3.5 and 5.6 yr, and over 88% in the 4-yr frequency band. Oscillatory modes of variance identified with singular spectrum analysis at ~3.5, 4.0, and 5.8 yr in both the instrumental and reconstructed series exhibit regimelike behavior over the 272-yr reconstruction. The tree-ring estimates also suggest a statistically significant increase in the interannual variability of winter SOI, more frequent cold events, and a slightly stronger sea level pressure gradient across the equatorial Pacific from the mid–nineteenth to twentieth centuries. Some of the variability in this reconstruction must be associated with background climate influences affecting the ENSO teleconnection to subtropical North America and may not arise solely from equatorial ENSO forcing. However, there is some limited independent support for the nineteenth to twentieth century changes in tropical Pacific climate identified in this reconstruction and, if substantiated, it will have important implications to the low-frequency dynamics of ENSO.

1. Introduction

Dramatic differences in the magnitude, persistence, and regional climatic impact of the El Niño–Southern Oscillation (ENSO) have been observed on annual and decadal timescales during the twentieth century (Allan et al. 1996). Dynamic models of ENSO have simulated major changes in the amplitude and frequency of warm and cold events on decadal timescales, but the reality and cause of this decadal aperiodicity are not clear (Cane et al. 1995). The decade-scale variance of ENSO may reduce the accuracy of climate and crop yield forecasts based in part on conditions in the equatorial Pacific (Phillips et al. 1996) and has stimulated inter-

*Tree-Ring Laboratory, University of Arkansas, Fayetteville, Arkansas.
+Tree-Ring Lab, Lamont-Doherty Earth Observatory, Palisades, New York.
#Climate Impact Group, CSIRO Mordialloc, Victoria, Australia.
@Geological Sciences/INSTAAR, University of Colorado, Boulder, Colorado.
&Department of Geology and Environmental Science, Stanford University, Stanford, California.
**Scripps Institute of Oceanography, LaJolla, California.
++Laboratory of Tree-Ring Research, The University of Arizona, Tucson, Arizona.
##Native Seed SEARCH, Tucson, Arizona.
@@INIFAP, San Luis Potosi, Mexico.
&&Byrd Polar Research Center, Ohio State University, Columbus, Ohio.
Corresponding author address: David Stahle, Tree-Ring Laboratory, Ozark Hall 108A, University of Arkansas, Fayetteville, AR 72701.
E-mail: dstahle@comp.uark.edu
In final form 21 May 1998.

est in the long-term behavior of the ENSO system. The instrumental meteorological and oceanographic records are not long enough to provide multiple realizations of decadal variability associated with ENSO. However, a number of annually resolved proxies of climate and oceanographic conditions have been discovered (e.g., Quinn et al. 1987; Thompson et al. 1984; Kennedy and Brassell 1992; Cole et al. 1993), and when found in climate regions influenced by ENSO these annually resolved proxies may help define the nature of ENSO variability in centuries prior to instrumental observations. Extended paleoclimatic estimates of ENSO may also help discriminate between possible causes of decadal variability in ENSO (Enfield and Cid 1991; Cane et al. 1995).

Ideally, exactly dated and climatically sensitive proxies from the equatorial Pacific centers of action of ENSO should be used to reconstruct the core characteristics of ENSO, and all remaining annual resolution proxies could then be used to map the spatial anomaly patterns of tropical and extratropical climate associated with each reconstructed warm and cold event (e.g., Rasmusson et al. 1995). Unfortunately, this ideal approach is barely possible even for the twentieth century due to the poor spatial coverage of instrumental data, particularly over the oceans, and is certainly impossible with the currently available network of exactly dated annually resolved paleoclimate proxies.

The reconstruction of tropical ENSO variability and the associated extratropical climate impact is further complicated by the fact that climate proxies are not uniformly accurate in recording their local climate or oceanographic environment. And the sometimes narrow seasonal response of even the most climate-sensitive proxies may not perfectly coincide with the seasonality of the local ENSO teleconnection. In spite of these limitations, we do have an excellent, massively replicated array of climate and ENSO-sensitive tree-ring chronologies for subtropical North America, and a recently confirmed and expanded tree-ring chronology of teak (*Tectona grandis*) from Java, Indonesia. These particular tree-ring data register the strongest and most stable ENSO signal yet detected in tree-ring chronologies worldwide. In this paper, we use these new and improved tree-ring data to develop a 272-yr reconstruction of the winter Southern Oscillation index (SOI) that reproduces the instrumental winter SOI variance with useful skill in the time, space, and frequency domains. We also discuss the strengths and limitations of this experimental reconstruction and consider how these paleo-ENSO estimates can be improved.

2. The Southern Oscillation index

A single comprehensive index of the Pacific basinwide air–sea interaction known as ENSO does not exist, but a number of reasonable approximations have been devised from the available meteorological and oceanographic measurements. The sea level pressure (SLP) records from Tahiti and Darwin, Australia, have been widely used to index the atmospheric pressure gradient across the tropical Pacific basin (e.g., Wright 1982; Jones 1988). A comprehensive reanalysis of the SLP data from Tahiti and Darwin has recently been completed, and a revised index of the Southern Oscillation (SO) has been developed based on the difference between SLP at Tahiti and Darwin for each month from 1876 to 1996 [i.e., this is a nonsmoothed version of the Troop SO index and is based on anomalies from the normalized mean difference series in standard deviation units ($\times$ 10); see Allan et al. (1996)]. In this analysis we have seasonalized three months December–February (DJF) of the Allan et al. (1996) data to construct a winter SOI (see appendix). This index targets the boreal (Northern Hemisphere) cool season, when warm and cold events typically mature in the equatorial Pacific, and represents the most reasonable seasonal window given the differing ENSO influence on the tree-ring data used in this analysis.

3. The proxy data

Hundreds of long, climatically sensitive tree-ring chronologies are available worldwide, but most are not well suited for ENSO reconstruction because they are confined to extratropical regions not strongly influenced by ENSO or do not respond to climate during the season of strongest ENSO influence. Annual tree-ring chronologies are extremely rare in the Tropics because the vast majority of tropical tree species do not produce anatomically distinctive annual growth rings in the absence of a pronounced winter dormant season. At present, no long-lived tree species are known to be useful for dendrochronology in Peru, Ecuador, or on the islands of the eastern or central Pacific. However, a very few tropical species with unequivocally annual growth rings have been identi-

fied in climates with dramatic seasonality in precipitation, and some may eventually prove as useful as the Javanese teak for paleoclimatic analyses of ENSO (e.g., Jacoby 1989; Buckley et al. 1995; Stahle et al. 1997).

The development of the teak chronology from Java (Fig. 1) is perhaps the most notable success for tropical dendrochronology thus far. Berlage (1931) was the first to develop a Javanese teak chronology, and his numerical chronology has been partially confirmed with new teak specimens from Java (D'Arrigo et al. 1994). The Saradan stand includes many trees over 200 yr old, and the derived chronology is well replicated from 1700 to 1995. The Saradan teak chronology is modestly correlated with the winter SOI for the period 1879–1977, both concurrently ($r = 0.19$; $P < 0.10$) and following the SOI by two seasons ($r = -0.35$; $P < 0.001$).

The huge network of extratropical tree-ring chronologies includes many series from the subtropics of Mexico and the southern United States where cool-season climate is influenced by ENSO (Fig. 1). Many of these excellent chronologies are significantly correlated with the winter SOI even though the growing season of the sample trees does not begin until spring or early summer. This ENSO teleconnection to tree growth exists because El Niño (La Niña) events during the boreal cool season tend to enhance (reduce) winter and early spring precipitation over subtropical North America (Ropelewski and Halpert 1987, 1989; Allan et al. 1996). This precipitation teleconnection has a very strong preconditioning effect on subsequent tree growth through the recharge (depletion) of soil moisture and may have a direct growth effect by enhancing cool season photosynthesis during moist El Niño years.

Tree-ring chronologies from subtropical North America have previously been used to reconstruct ENSO indices (Lough and Fritts 1985; Michaelsen 1989; D'Arrigo and Jacoby 1991, 1992; Stahle and Cleaveland 1993) or SSTs in regions sensitive to ENSO (e.g., Douglas 1980), but many new or updated chronologies have been added for this study. In particular, nine new earlywood-width chronologies of Douglas fir (*Pseudotsuga menziesii*), ponderosa pine (*Pinus ponderosa*), and pinyon pine (*P. edulis*) from Durango, Chihuahua, New Mexico, and southwestern Colorado were added to maximize the cool-season climate signal in tree growth. These earlywood- (or springwood) width chronologies are strongly correlated with "winter" precipitation (October–March), which is precisely the season of strongest ENSO influence on climate in this region. These nine earlywood chronologies, along with a few total ring-width chronologies of both ponderosa and pinyon pine from New Mexico and Arizona, and a network of nine post oak (*Quercus stellata*) chronologies from Texas and Oklahoma, exhibit the strongest simple correlations with ENSO indices of any presently available tree-ring chronologies worldwide (Fig. 2a). The ENSO teleconnection to tree growth in this region is consistent with the cool-season climate teleconnection and suggests that ENSO is an important forcing of interannual ecological rhythms in subtropical North America (e.g., Swetnam and Betancourt 1990). The tree growth correlation with winter SOI changes sign

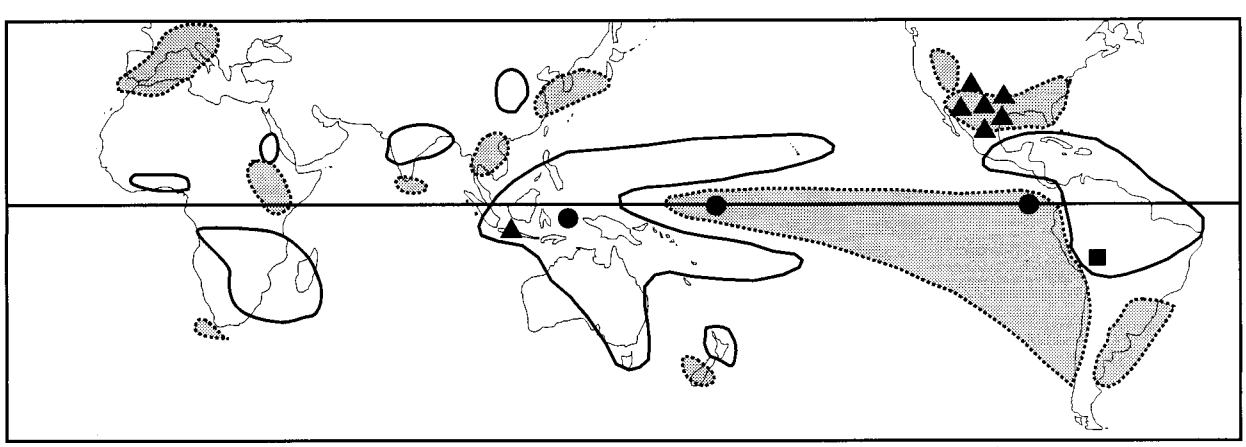

FIG. 1. General locations of the tree-ring, coral, and ice varve proxies used for experimental reconstructions of the winter SOI (triangles, circles, and squares, respectively). Several chronologies are represented by the triangles in North America. Regions with precipitation teleconnections to ENSO warm events are located (shading = wet anomalies; solid outline = dry anomalies; after Ropelewski and Halpert 1987, 1989; Allan et al. 1996).

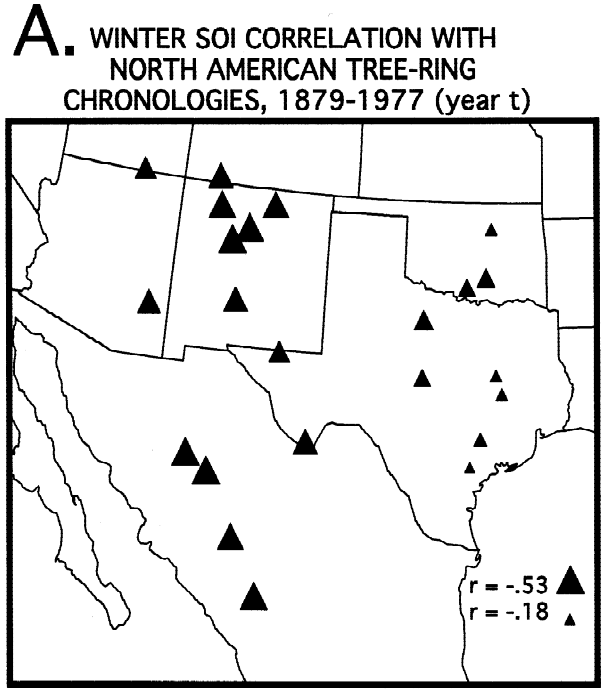

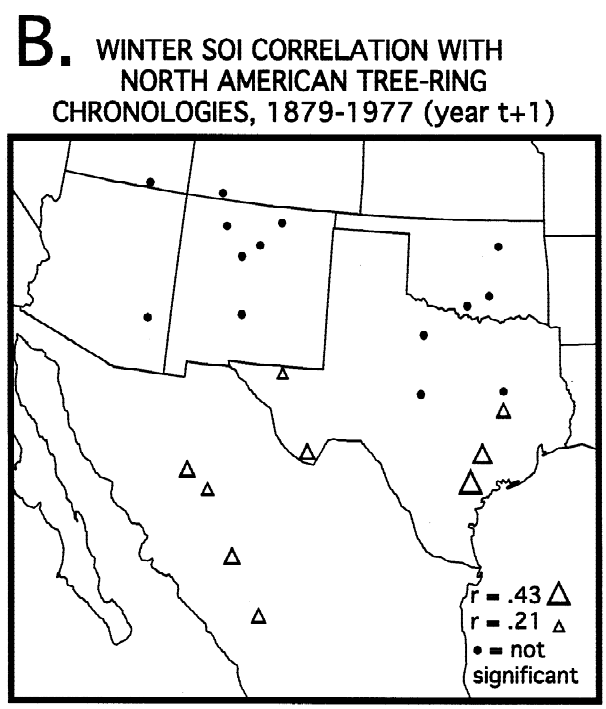

FIG. 2. The ENSO teleconnection to tree growth in subtropical North America for 1879–1977. Winter SOI was correlated with (a) tree-ring chronologies at these locations both concurrently (year *t*) and (b) with the tree-ring data lagging the SOI by 1 yr (year $t + 1$). The symbols are scaled by the magnitude of the correlation.

during the following year and is restricted to southern Texas and northern Mexico (Fig. 2b). This lagged response may only reflect the tendency for cold events to follow warm events (and vice versa), but it is spatially homogeneous, is present in both conifers and hardwoods, and adds to the SOI predictability of these proxies. Additional tree-ring chronologies from North and South America, New Zealand, Tasmania, and Zimbabwe were tested, but they did not improve upon the winter SOI estimation based solely on the data from subtropical North America and Indonesia.

Selected annual-resolution coral and ice core records available from the equatorial Pacific sector [i.e., $\delta^{18}O$ from corals at Urvina Bay in the Galapagos (1°S, 91°W; Dunbar et al. 1994), Tarawa (1°N, 172°E; Cole et al. 1993), and Bunaken (4°S, 124°E; M. D. Moore 1997, personal communication), and the ice core record of $\delta^{18}O$ from the Quelccaya ice cap, Peru (13°56′S, 70°50′W; Thompson et al. 1984)] were also used alone and in combination to develop experimental reconstructions of the winter SOI. The coral and ice core data available for this analysis are either relatively short (< 130 yr long) or are not well correlated with the particular seasonal index of the SO that is most coherent with the tree-ring data (e.g., the accumulation data from Quelccaya). For these reasons, we have based this experimental reconstruction of winter SOI solely on the tree-ring data and reserve the coral and ice core proxies for comparison with the tree-ring estimates. However, strong and highly significant correlations have been noted between certain coral records and ENSO (Cole et al. 1993), and between Quelccaya ice data and wind systems linked to ENSO. New coral, ice, and tree-ring records continue to be developed and together have great potential to improve and expand the annual-resolution reconstruction of ENSO and its associated climate teleconnections for the past two or three centuries.

4. Methods

Earlywood and total ring-width chronologies from Mexico, the southwestern United States, the southern Great Plains, and Java, Indonesia, were used to reconstruct the winter SOI (Table 1). A principal components (PC) regression scheme was used to calibrate the tree-ring time series with the instrumental winter SOI and to estimate winter SOI during the preinstrumental period (e.g., Cook and Kariukstis 1991; Cook et al. 1994). Three potential predictors of winter SOI were

derived for each tree-ring series by leading ($t-1$), synchronizing (t), and lagging ($t+1$) the proxy time series with respect to the instrumental SOI. This procedure seeks to accommodate known differences in the seasonal climate response of the tree-ring chronologies and in the seasonal timing and persistence of ENSO teleconnections to regional climate (e.g., Fig. 2). The various potential predictors of winter SOI were prewhitened and then again screened for significant correlation with the prewhitened winter SOI for year t ($p < 0.05$). Prewhitening the predictor and predictand variables is very important because the low-order persistence in tree-ring data can be quite strong, largely biological in origin, and unrelated to climate (Meko 1981). Prewhitening also improves the regression model linking tree rings to the SOI. All prewhitening was accomplished using low-order autoregressive models (Box et al. 1994) selected with the minimum Akaike information criterion (Akaike 1974). The 21 selected predictors (listed in Table 1) were then submitted to principal components analysis to identify a smaller number of orthogonal modes that represent most of the variance in the large array of 21 tree-ring variables. The first four PCs were retained based on the eigenvalue > 1.0 criterion, and together they represent 65% of the variance. The factor-score time series for these four selected eigenvectors were then regressed with the prewhitened winter SOI for the 1879–1977 calibration period in common with the winter SOI and all individual tree-ring chronologies.

TABLE 1. These beta weights provide a measure of the relative contribution of the original tree-ring chronologies to the reconstruction of winter SOI shown in Figs. 3 and 5. The species, chronology type, and lead-lag relationships of the tree-ring predictors with winter SOI are also listed (*PSME* = *Pseudotsuga menziesii*; *PIED* = *Pinus edulis*; *PIPO* = *P. ponderosa*; *QUST* = *Quercus stellata*; *TEGR* = *Tectona grandis*; EW = earlywood width; TRW = total ring width). With one exception, all North American predictor chronologies are either concurrent with winter SOI (t) or follow it by 1 yr ($t+1$). Only Ditch Canyon leads winter SOI ($t-1$). Because the Saradan teak chronology is calendar dated according to the year in which the October–March growing season begins, and winter (DJF) SOI is calendar dated by January, the $t+1$ linkage actually represents a relationship between teak growth beginning in October of the following year, 19 months after the end of the winter SOI season.

Tree-ring chronology	Species	Type	Lead lag	Beta weight
El Salto, Durango	*PSME*	EW	t	–0.0112
El Salto, Durango	*PSME*	EW	$t+1$	0.0403
Creel, Chihuahua	*PSME*	EW	t	–0.0775
Creel, Chihuahua	*PSME*	EW	$t+1$	0.0265
El Tabacote, Chihuahua	*PSME*	EW	t	–0.1080
El Tabacote, Chihuahua	*PSME*	EW	$t+1$	0.0222
Cerro Barajas, Durango	*PSME*	EW	t	–0.0908
Cerro Barajas, Durango	*PSME*	EW	$t+1$	0.0483
Navajo Mountain, Utah	*PIED*	TRW	t	–0.0184
Eagle Creek, Arizona	*PIED*	TRW	t	–0.0773
Pueblito Canyon, New Mexico	*PSME*	EW	t	–0.0651
Abouselman Springs, New Mexico	*PIPO*	TRW	t	–0.0399
Elephant Rock, New Mexico	*PIPO*	TRW	t	–0.0290
Paliza Canyon, New Mexico	*PIED*	TRW	t	–0.0383
Oscura Peak, New Mexico	*PIED*	TRW	t	–0.0623
Ditch Canyon, New Mexico	*PSME*	EW	$t-1$	0.0629
Ditch Canyon, New Mexico	*PSME*	EW	t	–0.0397
Post Oak PC1, Texas–Oklahoma	*QUST*	TRW	t	–0.0763
Post Oak PC1, Texas–Oklahoma	*QUST*	TRW	$t+1$	0.0423
Post Oak PC2, Texas–Oklahoma	*QUST*	TRW	$t+1$	–0.1644
Saradan Teak, Java, Indonesia	*TEGR*	TRW	$t+1$	–0.1778

The transfer function used to estimate winter SOI was derived by solving the multiple regression equation for each year from 1706 to 1977, with winter SOI designated as the dependent variable and the tree-ring eigenvector amplitude series as the "independent" variables. The autoregressive structure of the instrumental winter SOI was then added to the white noise time series of estimated winter SOI to complete the reconstructions [the instrumental winter SOI (1879–1977) was identified as an autoregressive (AR)-2 process representing 5.5% of the overall time series variance, with $t - 1$ and $t - 2$ coefficients of –0.043 and –0.233, respectively]. Adding in the AR-2 structure of the instrumental winter SOI assumes that the AR structure of the 1879–1977 period is representative of earlier years, which may not be entirely true. However, the resulting reconstruction is much more coherent with the instrumental SOI in the frequency domain than would be the case if AR modeling were not used in conjunction with the PC regression modeling.

A split period scheme was used to validate the tree-ring calibration against independent instrumental winter SO indices. The instrumental winter SO indices were split into two time series extending from 1879 to 1928 and from 1929 to 1977. The tree-ring data were then calibrated with PC regression (as above) against the instrumental SO indices during one subperiod, and the derived estimates were then compared with actual winter SOI during the alternate, statistically independent subperiod.

5. Results

The factor scores derived from the first four PCs of the North American and Javanese tree-ring data explain 53% of the winter SOI variance during the 1879–1977 calibration period (Fig. 3). The beta weights for each of the 21 original tree-ring variables included in the reconstruction are listed in Table 1 and measure the contribution of each individual variable to the final reconstruction of winter SOI. Split period calibration and verification tests (i.e., 1879–1928 and 1929–77, Table 2) indicate that the tree-ring predictors pass a battery of cross-validation statistics and are well correlated with independent winter SO indices not used to specify the calibration models. Investigations of the regression residuals indicate that the error of the full and split-period calibration models is normally distributed and free of significant short or long term autocorrelation [based on the Durbin–Watson test (Table 2) and the generalized autoregressive conditional heteroscedasticity (GARCH) model (SAS Institute 1993)]. This apparent randomness in the regression residuals from the reconstruction model is relevant to the interpretation of reconstructed changes in winter SOI variance (see discussion below).

The tree-ring estimates of winter SOI reproduce the timing of warm and cold events with reasonable fidelity but do not reproduce the full dynamic range of instrumental winter SOI (Fig. 3a). This truncation is in part the inevitable consequence of regression estimation and might be minimized with alternative quadratic or nonlinear estimation models. However, the key limitation remains the availability of long climate-sensitive proxies from the centers of action and primary teleconnection regions of ENSO worldwide.

The Javanese teak chronology has the highest single beta weight of the 21 tree-ring variables used in this reconstruction (Table 1), which underscores the importance of developing additional tree-ring chro-

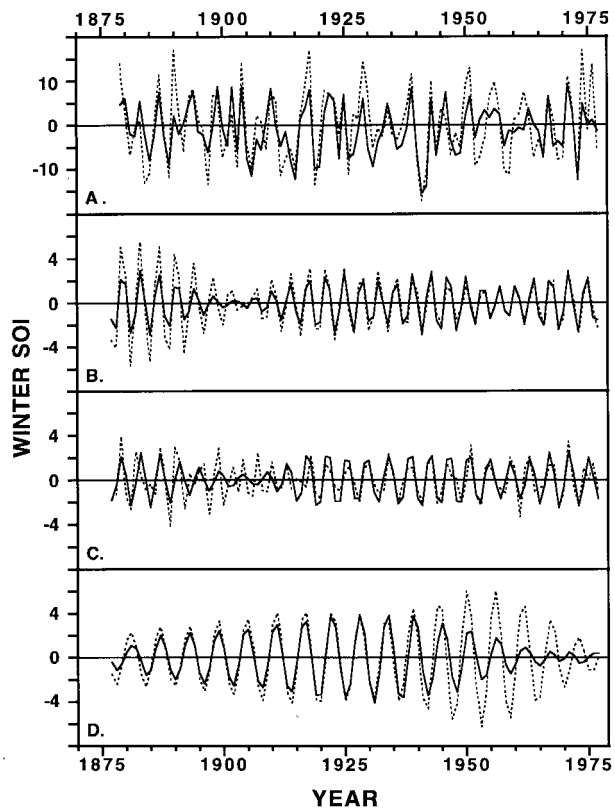

FIG. 3. (a) Observed (dashed line; appendix) and tree-ring reconstructed winter SOI (solid line) for the 1879–1977 calibration period (r^2adj = 0.53). The quasi 3.5-, 4.0-, and 5.8-yr waveforms identified in both the instrumental (dashed line) and the reconstructed data (solid line) are also plotted for the 1877–1977 common period [(b), (c), and (d), respectively].

nologies from the core region of ENSO. Surprisingly, however, experimental reconstructions of winter SOI using the regional subsets of tree-ring data as predictors indicate that the chronologies from subtropical North America are more strongly associated with winter SOI than the single teak chronology from Java, even though Java is under the western center of action of the SO. The Java chronology alone explains 11% of the winter SOI variance from 1879 to 1977, but the regional tree-ring data from Texas and Oklahoma, the southwestern United States, and Mexico individually explain 23%, 37%, and 36% of the winter SOI variance, respectively. This may simply reflect differences in the seasonal ENSO response of the Java series (the teak chronology is more highly correlated with June–December SOI) and the substantial replication of tree-ring proxies across subtropical North America.

Spatial correlation analysis was performed between instrumental and reconstructed winter SOI and gridded SSTs for the equatorial and North Pacific to assess the average strength of the large-scale ocean–atmosphere signal actually recorded by the tree-ring reconstruction (Figs. 4a,b,c). The instrumental Tahiti–Darwin winter SOI is negatively correlated with winter (DJF) season SSTs in the eastern equatorial Pacific and is positively correlated with SSTs in the western equatorial and North Pacific (Fig. 4a). This reflects the ocean–atmospheric coupling of ENSO, and the tree-ring reconstructed winter SOI reproduces this large-scale equatorial and North Pacific anomaly pattern with amazing detail (Fig. 4b). In fact, the correlations between reconstructed winter SOI and winter SSTs are slightly higher than the correlations based on the instrumental SO indices, in spite of the fact that the tree-ring estimates only explain 53% of the interannual variability of winter SOI.

The factor scores from the first PC of seven Douglas fir earlywood-width chronologies from Mexico and southwestern Texas were also correlated with the gridded SST data (Fig. 4c) to address the possibility that the tree-ring calibration with winter SOI somehow fitted the reconstructed SO indices to the SST anomaly pattern shown in Fig. 4a. Figure 4c demonstrates that the tree-ring data from Mexico and Texas strongly register the coupled air–sea system over the equatorial and North Pacific, even when the tree-ring data from Java and elsewhere in the southwestern United States are excluded from the analysis (the sign differences between Figs. 4c and 4a,b only reflect the sense of the ENSO teleconnection to climate over subtropical North America; in this case warm events are indicated by negative winter SO indices and are associated with wet winter/early spring conditions and positive tree growth in the Texas–Mexico sector). The strong SST signal in the raw tree-ring and reconstructed winter SO indices during the 1879–1977 cali-

TABLE 2. Calibration and verification statistics for the tree-ring reconstruction of winter SOI. The stability of the full calibration model based on the 1879–1977 time period (r^2adj = 0.53) was evaluated with two split-period calibration and verification experiments (1879–1928 and 1929–77). Here r^2adj = coefficient of determination adjusted for loss of degrees of freedom (Draper and Smith 1981). No significant autocorrelation was detected in the residuals from the models (i.e., Resid $r-1$) using the Durban–Watson statistic (Draper and Smith 1981).

Calibration			Verification					
Period	r^2adj	Resid r-1	Period	Corr.[a]	First diff corr.[b]	Means test[c]	Sign test[d]	RE[e]
1879–1928	0.58	0.11	1929–77	0.71*	0.81*	+0.31 ns	41/8*	0.50
1929–77	0.51	0.18	1879–1928	0.72*	0.80*	–0.30 ns	39/11*	0.52
1879–1977	0.53	0.15						

[a]Pearson correlation coefficient, r (Fritts et al. 1990).
[b]Pearson correlation coefficient after first-difference transformation of series (Fritts et al. 1990).
[c]Paired t-test of instrumental and reconstructed means (Steel and Torrie 1980). No significant difference is the desired outcome.
[d]Test of direction of reconstructed deviation from the instrumental mean (Fritts et al. 1990).
[e]RE = reduction of error test. Possible values range from +1.0 to $-\infty$. No test statistic is available, but any positive value indicates skill in reconstruction (Fritts et al. 1990).

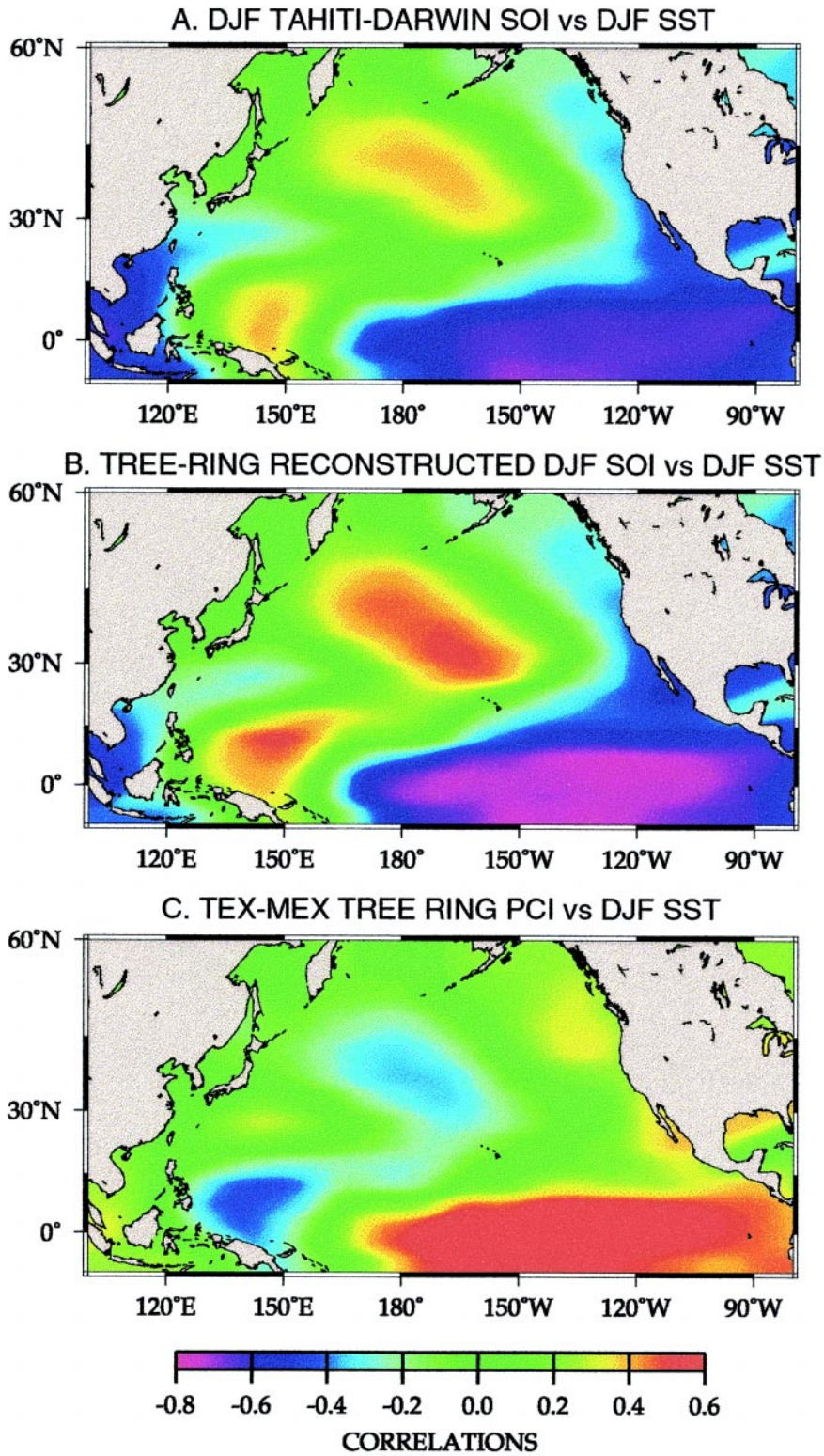

FIG. 4. Correlations between gridded SSTs (Kaplan et al. 1998) seasonalized to DJF and the instrumental (a) and tree-ring reconstructed (b) winter SOI for 1879–1977. The SSTs are also correlated with the factor scores on the first PC of earlywood tree growth in Mexico and southwestern Texas (c).

bration period indicates that the great air–sea interactions of ENSO over the equatorial and North Pacific are a dominant mode in the interannual variability of tree growth across subtropical North America and Indonesia. These results also suggest that the tree-ring data provide a reasonable proxy of the ENSO teleconnection to North America, if not of the core ENSO phenomenon itself (this uncertainty is examined in the discussion below). We assume, and the cross-validation experiments leave little reason to doubt (Table 2), that the tree-ring data are reasonable proxies of the winter SOI in the preinstrumental period as well.

Experimental calibrations between winter SOI and annually banded coral and ice core data indicate that the coral data have real potential to improve the tree-ring reconstruction of ENSO. The Tarawa and Bunaken data alone explain 41% and 23% of the winter SOI variance, respectively (although during slightly different calibration periods), even though winter (DJF) may not be the ideal season for the ENSO influence on these proxies. Nevertheless, calibration models for both coral sites can be verified against independent winter SO indices.

The Urvina Bay coral series is strongly linked with the winter SOI in the recent portion of the instrumental period (i.e., r^2adj = 0.41 for the 1929–77 period). However, the winter SOI linkage disappears during the earlier subperiod (1879–1928), which might reflect dating uncertainties that may be improved with recently developed coral data from the region. The

Quelccaya ice core alone could not be successfully calibrated with the winter SOI, which again must not be the ideal season because there is a strong link between $\delta^{18}O$ at Quelccaya and the easterly wind component at the 500-mb level, which is strongly modulated by SSTs in the eastern equatorial Pacific (e.g., Michaelsen and Thompson 1992).

The highest winter SOI calibration and verification statistics in these multiproxy experiments were obtained using the tree-ring predictors from subtropical North America and Java, along with coral predictors from Tarawa and Bunaken (r^2adj = 0.62 for 1894–1977). The Tarawa and Bunaken records are only 99 and 131 yr long, respectively, at present, but these experiments leave no doubt that improved estimates of past ENSO variability will be possible if longer coral series can be developed in the equatorial Pacific.

6. Analysis

The tree-ring reconstruction of winter SOI extends from 1706 to 1977 (Fig. 5a; see appendix) and at face value implies several interesting changes in the ENSO system over the past three centuries. Prolonged changes in winter SOI variance are reconstructed (Fig. 5a), including low variance around 1840 and higher variance after 1870. In particular, an increase in the frequency of winter SOI extremes after 1870 is evident in Fig. 6a, where the 272-yr reconstruction is plotted with the mean (−1.13) and the ±1.0 and ±2.0 standard deviation (std dev) thresholds (i.e., winter SOI = ±4.86 and ±9.72, respectively). Using the ≥ 1.0 std dev threshold to define cold events (i.e., winter SOI ≥ 3.73), there were only 22 cold events in the entire 173-yr period from 1706 to 1878, whereas 25 cold events were reconstructed for the 99 yr from 1879 to 1977 (an estimated cold event frequency of one per 7.86 and 3.96 yr, respectively). The frequency of reconstructed warm events (i.e., winter SOI ≤ −1.0 std dev, or ≤ −5.99) also increased after 1878, but not as dramatically as cold events (23 warm events from 1706 to 1878, 20 from 1879 to 1977, or 1 per 7.52 and 4.95 yr, respectively).

Ignoring for the moment questions concerning the true cause of these changes (see discussion below), we have investigated the possible statistical significance of the long-term changes in reconstructed winter SOI variance. We used the autoregressive conditional heteroscedasticity and GARCH models in the Autoreg Procedure (SAS Institute 1993) to test for variance

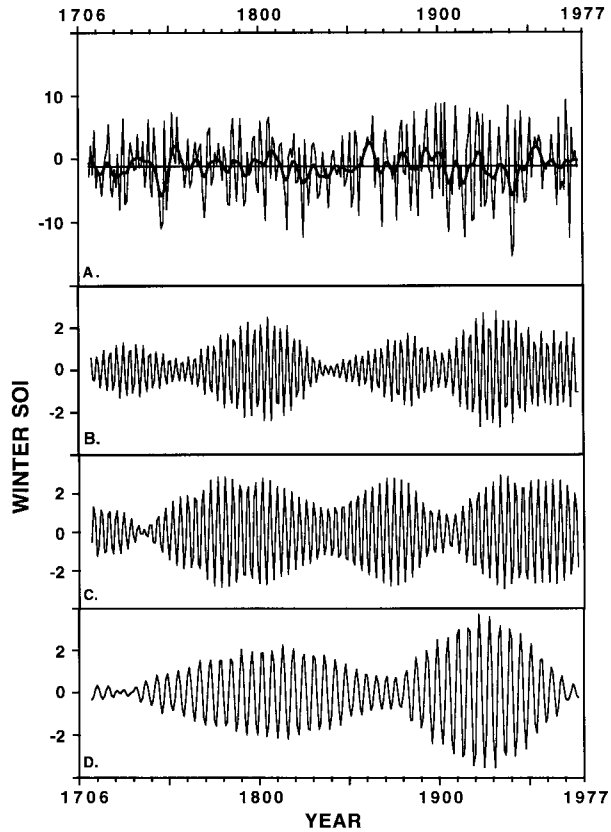

FIG. 5. (a) Tree-ring reconstructed winter SOI from 1706 to 1977 (see Fig. 3a; Tables 1, 2, 3; appendix). A smoothing spline was applied to emphasize the decadal variance in the reconstruction. The oscillatory modes of variance identified with singular spectrum analysis (SSA) at 3.53, 4.07, and 5.75 yr are also plotted [(b), (c), and (d), respectively].

trend in reconstructed winter SOI. The AR-2 structure of the reconstructed winter SOI was identified, and the associated random-shock time series was tested for heteroscedasticity for the period 1706–1977. Statistically significant autoregression out to order AR-12, and the significant GARCH1 term ($P < 0.01$) in the GARCH ($Q = 1$, $P = 1$) model suggest that the source of the heteroscedasticity in the random shock time series of reconstructed winter SOI is indeed a long-memory process. The GARCH estimates are normally distributed, which reinforces the statistical significance of the GARCH1 coefficient and the long memory conditional variance of reconstructed winter SOI. The conditional error variance from the GARCH model is plotted in Fig. 6b and indicates that the principal cause of the heteroscedasticity in the reconstruction is the twentieth-century period of relatively high variability evident in Figs. 5a and 6a. This is supported by the fact that no significant heteroscedasticity is evi-

dent when the reconstruction is tested just from 1706 to 1900.

The reconstruction also indicates a very small increase in the mean of winter SOI from the pre-instrumental to instrumental period (i.e., 1706–1878 mean = –1.23, 1879–1977 mean = –0.97). If real, this would suggest that the zonal pressure gradient across the equatorial Pacific has strengthened very slightly during the late nineteenth and twentieth centuries, which might reflect the reconstructed increase in the frequency of cold events after 1878.

Spectral and cross-spectral analyses (Jenkins and Watts 1968) indicate that the reconstruction is reproducing the variance of the instrumental winter SOI with considerable accuracy in the frequency domain (Figs. 7a,b,c; all analyses used a Hamming window and all significance tests were based on the highest-resolution spectra). The reconstructed winter SOI is coherent with the instrumental data at most frequencies between 2 and 10 yr, particularly in the ENSO frequency band at periods near 4.0 yr (Fig. 7a). The squared coherency plotted in Fig. 7a is analogous to the squared correlation between observed and reconstructed winter SOI in the frequency domain (Jenkins

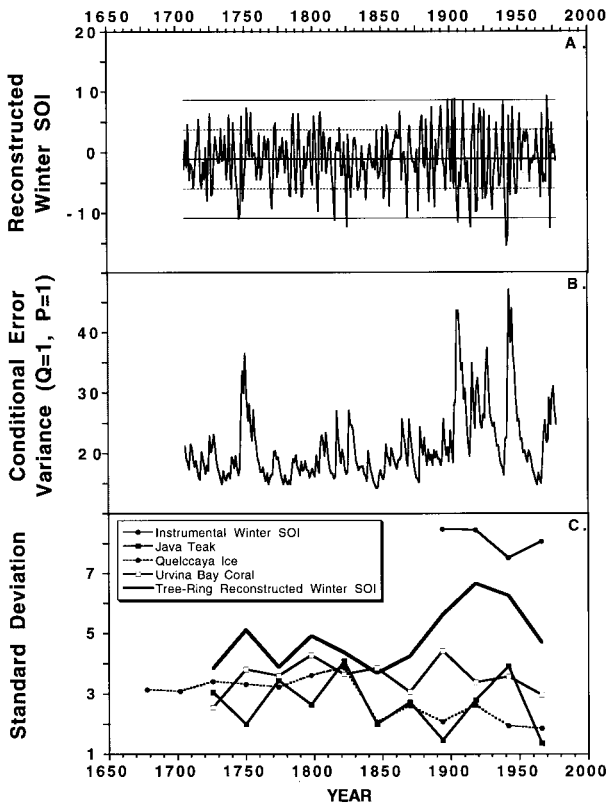

FIG. 6. (a) Reconstructed winter SOI, mean (–1.13), and the ±1.0 and ±2.0 standard deviation thresholds. (b) Conditional error variance from the GARCH (Q = 1, P = 1) model indicating long-term heteroscedasticity in reconstructed winter SOI. (c) The standard deviations of nonoverlapping 24-yr segments of instrumental winter SOI and four longer reconstructions are plotted for the midyear of each segment (which extend backward from 1977). The reconstructions of winter SOI based on the data from Java, Quelccaya, and Urvina Bay are not as strong as the full tree-ring reconstruction, but do suggest reduced variance in the nineteenth century (Quelccaya and Urvina Bay could not be verified, and the Java series verifies only weakly).

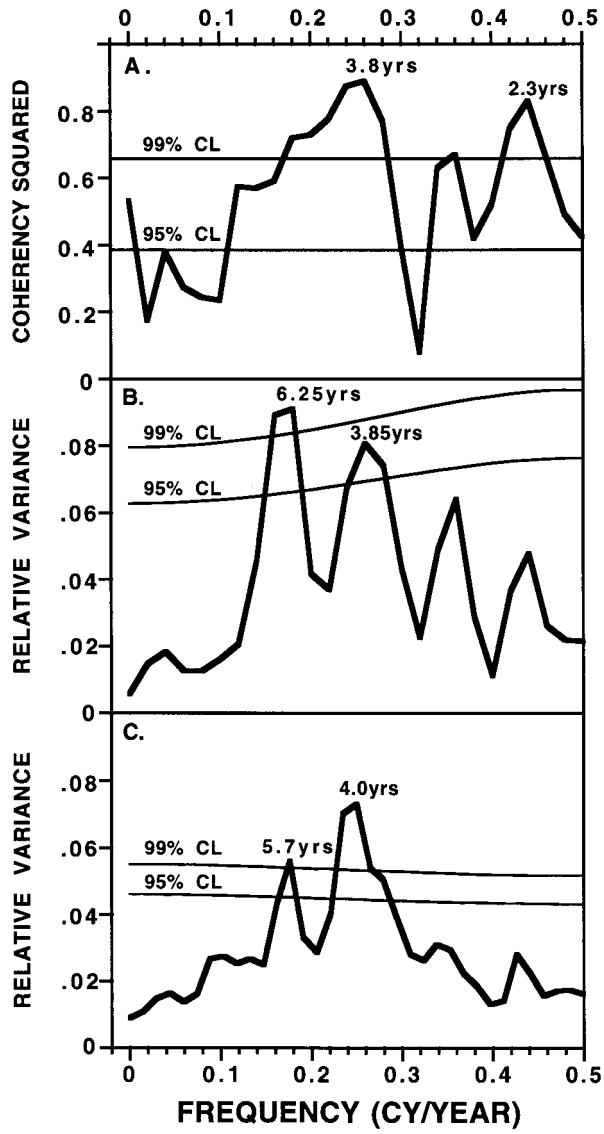

FIG. 7. (a) Coherency squared, computed between the observed and reconstructed winter SOI for the common period 1877–1977 [bandwidth (bw) = 0.05 cycles per year (cpy)]. (b) The spectral density of the instrumental winter SOI computed for the period 1877–1977 (bw = 0.05 cpy). (c) The spectral density computed for the reconstructed winter SOI for the period 1706–1977 (bw = 0.037 cpy).

and Watts 1968) and suggests that the reconstruction represents over 70% of the instrumental winter SOI variance in the frequency band between periods of 3.5 and 5.6 yr, and over 88% for periods between 3.85 and 4.17 yr (Fig. 7a). The reconstruction is in phase with the instrumental data at all frequencies except infinity (not shown).

The instrumental winter SOI has two significant spectral bands, peaking at 3.85 and 6.25 yr for the 1879–1977 time period, representing 15.6% and 18.3% of the overall winter SOI variance, respectively (Fig. 7b). These spectral peaks are both present in the full reconstruction from 1706 to 1977 (Fig. 7c), and when restricted to the 1879–1977 calibration period (not shown), but the 4-yr mode dominates. The strong peak from 3.58 to 4.25 yr represents 25.2% of the reconstruction variance, and the peak from 5.67 to 6.18 yr represents 10.24% (Fig. 7c).

Singular spectrum analysis (SSA; Voutard et al. 1992) identifies three important oscillatory modes of variance in the instrumental and reconstructed winter SOI, and these waveforms exhibit large-amplitude changes during the instrumental period (1877–1977) and over the full 272-yr reconstruction (1706–1977; Figs. 3 and 5; Table 3). SSA demonstrates that the reconstruction reproduces the oscillatory nature of the instrumental winter SOI at frequencies between 3.5 and 6.0 yr with reasonable fidelity (Fig. 3). In fact, the variance associated with each waveform is more consistent between the observed and reconstructed data (Table 3) than suggested by spectral analysis. A quasi-5.8-yr waveform is present in both observed and reconstructed data, but SSA resolves two additional waveforms at 3.5 and 4.0 yr with comparable variance in both datasets.

There is strong agreement in the timing of the observed and reconstructed waveforms plotted in Figs. 3b,c,d. The amplitude modulation of these waveforms is also largely coherent and in phase between the instrumental and reconstructed winter SOI. However, notable differences include the large amplitude of the observed 3.5-yr waveform before 1900 and the attenuation of the reconstructed 5.8-yr waveform after 1940 (Figs. 3b,d).

The three waveforms identified in the reconstructed winter SOI all exhibit substantial amplitude modulation over the past 272 yr (Figs. 5b,c,d). The amplitude of the quasi-5.8-yr reconstructed waveform increases dramatically in the early twentieth century, consistent with the changes observed in the instrumental SOI (Fig. 3d). The regimelike behavior of this reconstruction is consistent with a chaotic nonlinear model for long-term ENSO dynamics (Cane et al. 1995), but key ambiguities remain in the interpretation of this reconstruction (see below). These uncertainties must be minimized and the reconstructions improved and lengthened before these proxy estimates can be used with confidence to discriminate between models of long-term ENSO variability. Nonetheless, the available tree-ring data do provide promising empirical data on the low-frequency behavior of the ENSO system and can certainly be improved. The long tree-ring proxies might also be integrated with tropical coral and ice core records once the coral and ice chronologies are lengthened and (when doubts exist) exact calendar dating can be demonstrated.

7. Discussion

The tree-ring-reconstructed winter SO indices capture important aspects of ENSO variability in the time, space, and frequency domains. The reconstruction contains intriguing evidence for long-term changes in the ENSO system over the past three centuries. However, most of the tree-ring data were derived from the teleconnection province in subtropical North America. Also, the major change in reconstructed variance largely precedes the instrumental period and has not been specifically calibrated. Therefore, the true origin of the mid- to late-nineteenth century variance shift (Figs. 5a and 6a) remains unclear. There appear to be three possible explanations for the tree-ring recon-

TABLE 3. SSA waveforms identified in the full winter SOI reconstruction (1706–1977, m = 40, where m is the order of the autocorrelation matrix), and in observed and reconstructed winter SOI during the common period 1877–1977 (m = 30). The fraction of time series variance explained is also listed for each waveform.

	Dating	SSA waveforms (percent variance)		
Observed	1877–1977	3.53 (13.59%)	4.03 (12.31%)	5.77 (17.69%)
Reconstructed	1877–1977	3.53 (14.06%)	4.14 (14.29%)	5.90 (16.08%)
Reconstructed	1706–1977	3.53 (08.89%)	4.07 (14.25%)	5.75 (10.81%)

structed increase in winter SOI variance after 1870 (or some combination of the three).

1) The tree-ring proxies could be systematically biased prior to the calibration period. The reconstruction model relies heavily (though not exclusively; Table 1) on the tree-growth response in subtropical North America to wet conditions during El Niño years and dry conditions during La Niña years. However, this model does not uniquely fingerprint ENSO extremes because other circulation patterns can bring drought or wetness to the Texas–Mexico region. For example, the reconstruction indicates El Niño conditions during 1908 (−5.62), 1927 (−6.53), and 1930 (−5.26) when the actual winter SOI was 0.38, 2.58, and 7.18, respectively (Fig. 3a; see appendix). Consequently, the reconstructed changes in winter SOI variance might reflect changes in the degree to which the available tree-ring data uniquely fingerprint ENSO forcing. However, this potential flaw is not strongly evident during the calibration period from 1879 to 1977 when the residuals from the regression model linking winter SOI to tree growth have a random normal distribution.

Another possible source of proxy bias could arise from (undocumented) changes within the forest stands sampled for this study, which could have increased the variability, climatic sensitivity, and ENSO response of the sample trees after 1870. Anthropogenic impacts such as logging, grazing, or air pollution are obvious suspects. However, over 600 individual trees from 22 different forest stands in the United States, Mexico, and Java were utilized for this reconstruction. Most of these stands are quite remote and relatively undisturbed. It is highly unlikely that these conjectured forest changes would all operate in the same direction to increase variability of the resultant chronologies.

The coincidence of the variance shift near 1870 with the calibration period (1879–1977) also raises suspicion about the reconstruction, but a linear multiple regression model was used to calibrate the four PC factor scores of tree growth with the winter SOI. This linear transfer function will not introduce nonstationarities in variance that are not in the relative weighting of the four predictor time series. All of the regional tree-ring data from North America and Java exhibit an increase in variance from the nineteenth to twentieth century (not shown).

2) The strength of the ENSO teleconnection to subtropical North America where most of the tree-ring predictors are located could have increased after 1870, due to changes in the background climate and not ENSO. Teleconnection strength is certainly known to have wavered on decadal timescales for many areas influenced by ENSO (Allan et al. 1996), and this may reflect interference by midlatitude circulations that are not directly coupled with the energetics of the ENSO phenomenon itself. However, analyses of the ENSO influence on tree-ring reconstructed summer drought conditions indicate that the Texas–New Mexico sector retains the strongest and most stable ENSO signal for any portion of the continental United States during the instrumental period (Cole and Cook 1997). We also observe strong consistency of the ENSO signal in the Mexican earlywood-width chronologies during subperiods of the calibration period. This ENSO teleconnection to subtropical North America during winter reflects a strong dynamical link between anomalous convection in the central and eastern Pacific via the enhanced subtropical jet (e.g., Barnett 1981). Individual cloud surges originating along the ITCZ near Fanning Island in the central Pacific have been tracked across northern Mexico and into Florida on this vigorous low-latitude flow during warm events (Douglas and Englehart 1981). Nevertheless, the ENSO teleconnection to subtropical North America is not perfectly stable, and some of the variability in the tree-ring reconstruction of winter SOI certainly must reflect changes in the background climate over North America, particularly at frequencies above or below the highly coherent period of 4.0 yr.

3) The reconstructed increase in winter SOI variance after 1870 could reflect a true change in the ENSO system itself over the equatorial Pacific and consequently its teleconnected influence to climate over subtropical North America. There is some independent evidence for a mid- to late-nineteenth century shift in the interannual variability of climate over the tropical Pacific. These records are far from complete or unequivocal, but they do offer limited support for the reconstructed changes in the nineteenth century, and suggest that these changes may not have been the sole function of teleconnection strength to North America.

First, Rasmusson et al. (1995) identify century-scale changes in the intensity of the ENSO cycle in selected instrumental SST and SLP data from the Tropics, with high variance in the late-nineteenth and early twentieth centuries, and lower variance by 1930. The standard deviation of nonoverlapping 24-yr segments of the instrumental winter SOI parallels these trends (Fig. 6b).

Second, the reconstructed winter SOI and its GARCH model of conditional error variance are plot-

ted (Figs. 6a,b) along with the standard deviations for 24-yr segments of the reconstruction and three additional winter SOI reconstructions based only on the Java teak chronology, the Quelccaya ice core, and the Urvina Bay coral (Fig. 6c). These latter three proxies do not individually explain large fractions of winter SOI variance, but all were recovered from the equatorial Pacific sector, all contain at least a weak ENSO signal, and all exhibit a degree of reduced variance in the mid–nineteenth century (Fig. 6c).

Third, Enfield and Cid (1991) identified a decreased frequency of strong ENSO events in the nineteenth century, based on analyses of historical records compiled by Quinn et al. (1987). The longer recurrence interval for strong events in the mid–nineteenth century in the Quinn et al. (1987) record parallels the similar shift noted in the Urvina Bay coral (Dunbar et al. 1994). Enfield and Cid hypothesize that the recurrence interval for ENSO events may fluctuate between 3 and 4 yr in possible response to solar forcing of the quasi-biennial oscillation of stratospheric winds. The relatively low variance of tree-ring reconstructed winter SOI (Figs. 5a and 6a) during much of the nineteenth century is consistent with the historical and coral evidence for longer return intervals between strong events, and the SSA resolution of the quasi-3.5- and 4.0-yr waveforms in both the instrumental and reconstructed winter SOI (Table 3) must reflect the tendency for recurrence intervals to fluctuate between 3 and 4 yr.

Fourth, a recent tree-ring reconstruction of the summer Trans Polar Index of midlatitude circulation over the Southern Ocean (Villalba et al. 1997) contains a strong ENSO-band frequency peak and is coherent with the instrumental SOI at wavelengths around 3.4–3.6 yr for the interval 1866–1984. The amplitudes of the 3–4-yr waveforms derived from these data were also substantially reduced during the nineteenth century (Villalba et al. 1997).

8. Conclusions

These multiproxy comparisons, though far from final, tentatively suggest that the envelope of ENSO variance, and not just the regional teleconnection to subtropical North America, may have increased from the nineteenth to twentieth century. The reconstruction also indicates a very slight increase in the zonal pressure gradient across the equatorial Pacific during the period 1879–1977 (i.e., more positive winter SO indices and more frequent cold events, compared with the 1706–1878 time period), which would be consistent with the observed decrease in SSTs in the eastern equatorial Pacific during the twentieth century (Cane et al. 1997). If these reconstructed nineteenth to twentieth century changes in reconstructed winter SOI are substantiated by further studies, they will have important implications to the long-term dynamics of ENSO and its associated climate teleconnections.

Our experiments suggest that the development of longer coral records from the tropical Pacific and additional tree-ring chronologies from the western tropical Pacific should help to substantially improve on this tree-ring reconstruction of the SO. The voluminous multilingual historical archives also have tremendous potential for reconstructing past ENSO activity. The archival chronology of past ENSO events compiled by Quinn et al. (1987) has been criticized, especially the degree to which historical citations for conditions in the coastal zone of Peru and Ecuador represent fully coupled basinwide ENSO anomalies (e.g., Rasmusson et al. 1995). Indeed, we find only limited agreement between the tree-ring reconstructed winter SOI (Fig. 5a) and the Quinn et al. (1987) chronology of warm events [i.e., 28 of 40 strong to very strong warm events identified by Quinn et al. (1987) for the period 1706–1977 were reconstructed as negative winter SO indices, and the reconstructed mean SOI for these 40 yr was –2.93]. Nevertheless, historical references to environmental conditions in the western equatorial Pacific and the global Tropics remain an extremely promising, exactly dated, and surprisingly underutilized source of information on past ENSO extremes.

The sparse network of exactly dated, annual-resolution ENSO proxies now available is reminiscent of the circumstances surrounding Sir Gilbert Walker's investigations of the SO early this century. Walker did not enjoy the globally representative SST and sea level pressure fields, nor the tropical Pacific products of Tropical Ocean Global Atmosphere/Thermal Arraying the Ocean (TOGA/TAO) or the Ocean Topography Experiment (TOPEX/Poseidon). But he did use what climatological data were available to index the SO, including such widespread data as Samoa pressure, Charleston, South Carolina, pressure, Java rainfall, and much more (Allan et al. 1996) to describe what is now recognized as the atmospheric component of the most important cause of interannual climatic variability on earth. The network of ENSO-sensitive proxies is in its infancy. It is not ideally distributed and will have to be improved with further research. Nevertheless, the available tree-ring data from subtropi-

cal North America and Java have a demonstrable temporal and spatial signal of ENSO, and the derived reconstruction is particularly strong in the 4-yr frequency band. The aperiodic regimelike behavior evident in the reconstructed quasi-4-yr waveform of winter SOI has important implications for the low-frequency dynamics of ENSO and strongly justifies further development of annual paleoclimatic proxies of the ENSO system.

Acknowledgments. We thank Professor James E. Dunn, David M. Meko, Rachel Krusic, Armando Rodriquez, Wilbur Salinas, Gene Paull, Gordon C. Jacoby, Malcolm K. Hughes, Rex Adams, Peter Z. Fule, Thomas P. Harlan, Thomas H. Naylor (deceased), three anonomous reviewers for helpful suggestions, the Instituto Nacional de Investigaciones Forestales y Agropecuarias (S.L.P., Mexico), and the Indonesian Institute of Sciences (LIPI). This research was supported by grants from the National Science Foundation (Grants ATM-9528148 and ATM-9705676) and the National Oceanic and Atmospheric Administration (Grant NA56GPO217). RJA was supported under the CSIRO Climate Change Research Program, funded partially by the Australian Commonwealth Department of Environment, Sport, and Territories, and the State Governments of Northern Territory, Queensland, and Western Australia. This is Lamont-Doherty Earth Observatory contribution number 5852.

Appendix: Reconstructed and observed winter SOI (Appendix appears as a table on the adjacent page)

References

Akaike, H., 1974: A new look at the statistical model identification. *IEEE Trans. Auto. Control,* **AC-19,** 716–723.

Allan, R. J., J. Lindesay, and D. Parker, 1996: *El Niño/Southern Oscillation & Climatic Variability*. CSIRO Publishing, 408 pp.

Barnett, T. P., 1981: Statistical prediction of North American air temperatures from Pacific predictors. *Mon. Wea. Rev.,* **109,** 1021–1041.

Berlage, H. P., 1931: On the relationship between thickness of tree rings of Djati (teak) trees and rainfall on Java (in Dutch). *Tectona,* **24,** 939–953.

Box, G. E. P., G. M. Jenkins, and G. C. Reinsel, 1994: *Time Series Analysis, Forecasting and Control.* Prentice Hall, 575 pp.

Buckley, B. M., M. Barbetti, M. Watanasak, R. D'Arrigo, S. Boonchirdchoo, and S. Sarutanon, 1995: Dendrochronological investigations in Thailand. *IAWA J.,* **16,** 393–409.

Cane, M. A., R. G. Fairbanks, and G. T. Shen, 1993: Recent variability in the Southern Oscillation: Isotopic results from a Tarawa atoll coral. *Science,* **260,** 1790–1793.

——, S. E. Zebiak, and Y. Xue, 1995: Model studies of the long-term behavior of ENSO. *Natural Climate Variability on Decade-to-Century Time Scales,* Climate Research Committee, Eds., National Academy Press, 442–457.

——, A. C. Clement, A. Kaplan, Y. Kushnir, D. Pozdnyakov, R. Seager, S.E. Zebiak, and R. Murtugudde, 1997: Twentieth-century sea surface temperature trends. *Science,* **275,** 957–960.

Cole, J. E., and E. R. Cook, 1997: The coupling between ENSO and US drought: How stable is it over the past century? *Proc. AGU Fall Meeting,* San Francisco, CA, Amer. Geophys. Union.

Cook, E. R., and L. Kairiukstis, 1991: *Methods of Dendrochronology: Applications in the Environmental Sciences.* Kluwer, 163–217.

——, K. R. Briffa, and P. D. Jones, 1994: Spatial regression methods in dendroclimatology: A review and comparison of two techniques. *Int. J. Climatol.,* **14,** 379–402.

D'Arrigo, R. D., and G. C. Jacoby, 1991: A thousand year record of northwestern New Mexico winter precipitation reconstructed from tree rings and its relation to El Niño and the Southern Oscillation. *Holocene,* **1/2,** 95–101.

——, and ——, 1992: A tree-ring reconstruction of New Mexico winter precipitation and its relation to El Niño/Southern Oscillation events. *El Niño: Historical and Paleoclimatic Aspects of the Southern Oscillation,* V. Markgraf and H. Diaz, Eds., Cambridge University Press, 243–257.

——, ——, and P. J. Krusic, 1994: Progress in dendroclimatic studies in Indonesia. *Terr. Atmos. Oceanic Sci.,* **5,** 349–363.

Douglas, A. V., 1980: Geophysical estimates of sea-surface temperatures off western North America since 1671. California Cooperative Oceanic Fisheries Investigations Rep. 21, 112 pp.

——, and P. J. Englehart, 1981: On a statistical relationship between autumn rainfall in the central equatorial Pacific and subsequent winter precipitation in Florida. *Mon. Wea. Rev.*, **109,** 2377–2382.

Draper, N. R., and H. Smith, 1981: *Applied Regression Analysis.* 2nd ed. John Wiley and Sons, 709 pp.

Dunbar, R. B., G. M. Wellington, M. W. Colgan, and P. W. Glynn, 1994: Eastern Pacific sea surface temperature since 1600 A.D.: The δ^{18}O record of climate variability in Galapagos corals. *Paleooceanography,* **9,** 291–315.

Enfield, D. B., and L. Cid, 1991: Low-frequency changes in El Niño–Southern Oscillation. *J. Climate,* **4,** 1137–1146.

Fritts, H. C., J. Guiot, and G. A. Gordon, 1990: Verification. *Methods of Dendrochronology: Applications in the Environmental Sciences,* E.R. Cook and L.A. Kariukstis, Eds., Kluwer, 178–185.

Jacoby, G. C., 1989: Overview of tree-ring analysis in tropical regions. *IAWA Bull.,* **10,** 103–108.

Jenkins, G. M., and D. G. Watts, 1968: *Spectral Analysis and Its Applications.* Holden-Day, 525 pp.

Jones, P. D., 1988: The influence of ENSO on global temperatures. *Climate Monitor,* **17,** 80–89.

Kaplan, A., M. Cane, Y. Kushnir, A. Clement, M. Blumenthal, and B. Rajagopalan, 1998: Analyses of global sea surface temperature 1856–1991. *J. Geophys. Res.,* **103**, 18 567–18 589.

Kennedy, J. A., and S. C. Brassell, 1992: Molecular records of twentieth-century El Niño events in laminated sediments from the Santa Barbara basin. *Nature,* **357,** 62–64.

Lough, J. M., and H. C. Fritts, 1985: The Southern Oscillation and tree rings: 1600–1961. *J. Climate Appl. Meteor.*, **24,** 952–966.

Meko, D. M., 1981: Applications of Box–Jenkins methods of time series analysis to the reconstruction of drought from tree rings. Ph.D. dissertation, University of Arizona, 149 pp.

TABLE A1. The tree-ring reconstructed winter SOI from 1706 to 1977 (top), and the Allan et al. (1996) winter SOI for 1876–1996 (bottom, with mean of 0.0 for 1879–1977).

Date	0	1	2	3	4	5	6	7	8	9
1706							–2.74	2.02	–2.45	4.55
1710	–4.54	–1.84	–2.56	–5.82	–2.75	0.04	1.46	5.45	–4.63	–5.91
1720	–1.64	–4.42	0.81	–8.02	–1.09	6.29	–7.09	–6.68	–0.63	2.54
1730	0.65	–1.73	–1.53	3.91	–1.37	–1.05	2.71	–4.43	–1.71	6.19
1740	–3.94	–5.90	4.89	0.95	–3.70	–6.38	–10.93	–9.92	6.00	–7.92
1750	–3.80	–1.08	7.31	0.90	–0.65	6.55	–0.80	–0.03	–0.31	–4.42
1760	–2.41	3.13	–4.50	–3.42	0.33	2.62	–0.94	1.40	2.31	–5.07
1770	–9.21	–4.91	4.02	4.85	–4.09	–2.81	0.98	–0.90	2.42	–0.41
1780	–3.33	1.91	–0.39	–7.08	–7.26	3.77	6.34	–1.97	–6.66	0.14
1790	6.36	–1.27	–7.33	–6.52	1.00	–2.53	–1.85	3.03	3.55	–4.09
1800	–5.29	5.96	2.29	–4.69	–9.67	5.60	6.62	–3.01	3.36	2.31
1810	–3.36	–1.43	2.11	2.42	–2.88	–5.84	–11.17	0.30	1.56	0.25
1820	3.96	–3.78	–3.57	1.67	–3.95	–12.29	3.02	–2.45	–7.34	–2.81
1830	1.99	2.46	0.57	–6.17	–5.61	–3.33	1.04	–2.77	–1.59	–7.74
1840	–3.03	0.20	1.28	–1.53	–2.47	–1.24	–2.84	3.59	–4.27	–3.52
1850	–2.07	4.07	–7.53	–5.48	4.46	3.13	–8.87	0.29	–1.20	1.42
1860	1.95	3.44	2.35	2.31	6.70	–4.46	–0.32	0.08	–3.52	–10.66
1870	2.31	4.43	0.18	–1.51	–1.50	–3.26	0.45	–9.61	–0.88	4.67
1880	6.05	–2.01	–2.50	5.36	–2.04	–8.08	–2.06	7.37	–2.98	–8.92
1890	2.09	–2.00	0.35	4.61	7.67	–1.37	–2.23	–6.24	–0.67	8.70
1900	–0.49	–4.74	8.64	–5.86	8.79	–7.50	–11.51	–3.30	–5.62	1.15
1910	8.35	–0.18	–4.82	–1.52	–7.76	–12.31	1.42	3.74	7.96	–9.77
1920	–9.45	2.88	7.22	5.52	–7.60	6.98	–7.50	–6.53	–1.32	5.97
1930	–5.26	–9.43	–3.78	–1.19	4.86	0.23	–5.49	–4.56	–0.51	8.32
1940	–5.66	–15.43	–13.71	5.97	–6.96	–0.30	7.43	–3.43	–6.87	–6.39
1950	1.88	6.38	–2.92	1.23	3.33	1.73	3.57	2.37	–4.79	–1.26
1960	–1.75	–0.64	–1.24	3.74	0.09	–1.45	–7.40	6.42	–4.90	–3.71
1970	–4.86	9.22	2.60	–12.50	4.81	–0.14	1.16	–1.38		

Date	0	1	2	3	4	5	6	7	8	9
1876							9.98	–8.22	–16.52	13.88
1880	2.68	–6.72	–0.92	1.08	–13.02	–11.02	0.48	11.28	–1.62	–11.72
1890	16.88	2.38	–6.02	6.08	8.18	1.28	–0.82	–13.52	6.48	7.38
1900	–7.42	–2.62	2.48	–9.42	14.28	–4.92	–10.12	2.18	0.58	–5.62
1910	7.18	5.48	–11.52	–7.52	–5.22	–10.12	2.28	8.98	16.98	–13.42
1920	–4.92	7.78	7.08	5.88	–2.32	6.88	–11.12	2.58	1.38	14.18
1930	7.18	–5.22	–0.72	–2.52	3.38	–2.02	–3.52	–0.22	4.38	11.58
1940	–6.22	–17.12	–10.32	9.98	–6.02	3.68	1.38	–6.72	–1.82	–5.32
1950	8.78	12.98	–9.32	–7.22	–2.92	6.48	9.68	2.68	–10.42	–11.32
1960	1.18	2.28	7.38	3.08	–7.42	–3.32	–6.42	6.48	1.08	–7.92
1970	–7.52	10.88	2.98	–11.72	16.88	–1.02	13.48	–6.22	–15.12	–0.92
1980	–2.72	–2.32	3.28	–31.12	0.78	–1.12	–2.12	–13.02	–3.32	9.68
1990	–10.12	–0.62	–19.32	–9.12	–1.42	–8.12	–0.42			

Michaelsen, J., 1989: Long period fluctuations in El Niño amplitude and frequency reconstructed from tree rings. *Aspects of Climate Variability in the Pacific and the Western Americas, Geophysical Monograph*, No. 55, Amer. Geophys. Union, 69–74.

——, and L. G. Thompson, 1992: A comparison of proxy records of El Niño/Southern Oscillation. *El Niño, Historical and Paleoclimatic Aspects of the Southern Oscillation,* H. F. Diaz and V. Markgraf, Eds., Cambridge University Press, 323–348.

Phillips, J. G., C. Rosenzweig, and M. Cane, 1996: Exploring the potential for using ENSO forecasts in the U.S. Corn Belt. *Drought Network News,* **8,** 6–10.

Quinn, W. H., V. T. Neal, and S. E. Antunez de Mayolo, 1987: El Niño occurrences over the past four and a half centuries. *J. Geophys. Res.,* **92** (C13), 14 449–14 461.

Rasmusson, E. M., X. Wang, and C. F. Ropelewski, 1995: Secular variability of the ENSO cycle. *Natural Climate Variability on Decade-to-Century Time Scales,* Climate Research Committee, Eds., National Academy Press, 458–469.

Ropelewski, C. F., and M. S. Halpert, 1987: Global and regional scale precipitation patterns associated with the El Niño/Southern Oscillation. *Mon. Wea. Rev.,* **115,** 1606–1626.

——, and ——, 1989: Precipitation patterns associated with the high phase of the Southern Oscillation. *J. Climate,* **1,** 172–182.

SAS Institute Inc., 1993: *SAS/ETS User's Guide, Version 6.* 2d ed. SAS Institute Inc., 890 pp.

Stahle, D. W., and M. K. Cleaveland, 1993: Southern Oscillation extremes reconstructed from tree-rings of the Sierra Madre Occidental and southern Great Plains. *J. Climate,* **6,** 129–140.

——, ——, G. A. Haynes, J. Klimowicz, P. Mushove, P. Ngwenya, and S. E. Nicholson, 1997: Development of a rainfall sensitive tree-ring chronology in Zimbabwe. Preprints, *Eighth Symp. on Global Change Studies,* Long Beach, CA, Amer. Meteor. Soc., 205–211.

Steel, R. G. D., and J. H. Torrie, 1980: *Principles and Procedures of Statistics: A Biometrical Approach.* 2d ed. McGraw-Hill, 633 pp.

Swetnam, T. W., and J. L. Betancourt, 1990: Fire–Southern Oscillation relations in the southwestern United States. *Science,* **249,** 1017–1020.

Thompson, L. G., E. Mosley-Thompson, and B. M. Arnao, 1984: El Niño/Southern Oscillation events recorded in the stratigraphy of the tropical Quelccaya ice cap, Peru. *Science,* **226,** 50–53.

Villalba, R., E. R. Cook, R. D. D'Arrigo, G. C. Jacoby, P. D. Jones, M. J. Salinger, and J. Palmer, 1997: Sea level pressure variability around Antarctica since A.D. 1750 inferred from subantarctic tree-ring records. *Climate Dyn.,* **13,** 375–390.

Voutard, R., P. Yiou, and M. Ghil, 1992: Singular spectrum analysis: A toolkit for short noisy chaotic time series. *Physica D,* **58,** 95–126.

Wright, P. B., 1982: Homogenized long-period Southern Oscillation indices. *Int. J. Climatol.,* **9,** 33–54.